Estimation of Voltage Regulator Stable Region Using Radial Basis Function Neural Network

Mohd Hairi Mohd Zaman, M Marzuki Mustafa and Aini Hussain
Department of Electrical, Electronic and Systems Engineering, Faculty of Engineering and Built Environment
Universiti Kebangsaan Malaysia, 43600 Bangi, Selangor, Malaysia
hairizaman@ukm.edu.my

***Abstract*—Disturbance to the voltage regulator (VR) output caused by the abrupt change in load current can be compensated using an output capacitor with an internal parasitic element called the equivalent series resistance (ESR). However, the ESR value changes due to aging and temperature change factors, thereby creating a VR stable region in terms of ESR. In practice, time-consuming and high-expertise manual characterization is required to characterize the VR stable region during the design and manufacturing phases. Therefore, this research aims to develop an efficient and effective VR characterization method. In this work, the radial basis function neural network (RBFNN) approach was implemented to estimate the stable region. Results show that the RBFNN approach yields a stable region with higher estimation accuracy and faster characterization time than those of manual characterization. VR characterization using the RBFNN approach can efficiently and effectively estimate the VR stable region.**

***Index Terms*—Equivalent Series Resistance; Output Capacitor; Radial Basis Function; Voltage Regulator Stable Region Characterization.**

I. Introduction

Voltage regulator (VR) is a power converter component in most electronic products. This component converts the unstable and noisy input voltage and current to a stable and load-independent output supply [1]. Thus, VR stability is an important requirement in VR design [2, 3]. This requirement eventually requires accurate characterization during VR manufacturing [4] in terms of the physical parameter that may cause VR output instability.

Disturbance to the VR output that causes instability is mainly due to the abrupt change in load current. In many cases, the disturbance can be compensated using an output capacitor [1, 5, 6]. This capacitor possesses an internal parasitic resistive element called the equivalent series resistance (ESR) [7]. ESR plays an important role in disturbance compensation by adding a significant pole and zero in the output impedance transfer function of VR [6, 8]. The ESR value, however, changes due to aging and temperature change factors [9], thereby creating a VR stable region in terms of ESR. A work has been conducted to determine the stable or failure region for analog circuits [10]. Therefore, this stable region needs to be accurately characterized over a range of ESR and output current during the design and manufacturing phases.

The performance of each manufactured VR varies due to variation in the manufacturing process. As such, time-consuming and high-expertise manual VR characterization is required to obtain an accurate, stable region. An actual VR model is difficult to be determined even if the initial design is known. Therefore, the main objective of this research is to develop an efficient and effective characterization of VR stable region in terms of ESR.

II. Material and Methods

This research involves two main phases: the development of the stable region and that of the new VR characterization method in terms of ESR. First, a stable region benchmark, including ESR specification limit, was developed on the basis of the outcomes of manual characterization. Second, the newly proposed characterization method, which can be categorized as a fully data-driven (FDD) approach, was developed. The FDD approach utilized the radial basis function neural network (RBFNN) approach to estimate the stable region. This approach will be further described in the subsequent section.

A. Characterization of VR Stable Region

Characterization of VR stable region in terms of ESR involves the detailed analysis of VR output stability over a range of ESR and output current. This characterization process measures the VR circuit output performance, such as overshoot and undershoots, and then decides whether the measured performance is stable or unstable. In this study, these processes were iteratively executed until all operating points were completed. Then, the overall outcomes of VR characterization were summarized in a special graph called ESR tunnel graph. Figure 1 shows an example of the ESR tunnel graph for a VR model of TPS763XX series from Texas Instruments [11]. This graph indicates the stable and unstable regions that are separated by the stability boundaries.

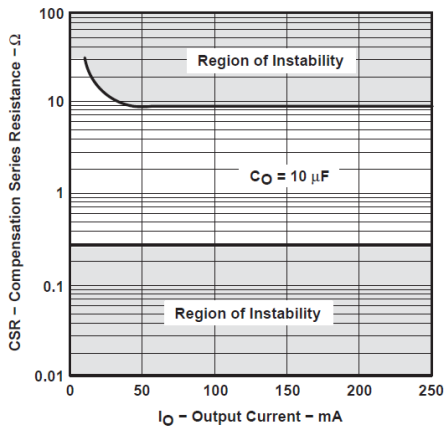

Figure 1: Example of ESR tunnel graph for VR model series TPS763XX from Texas Instruments

B. Test Circuit Development

Figure 2 shows the test circuit developed in this work. This circuit is a small signal equivalent circuit based on the VR model of TPS763XX series from Texas Instruments. Figure 1 shows that a stable region is located between two unstable regions, thereby creating two separated stability boundaries. Thus, two ESR specification limits are found, which indicates that the ESR value cannot be too low or too high. In this work, the test circuit was simulated in ORCAD software from Cadence. Further analysis was then implemented in MATLAB software from Mathworks with Neural Network Toolbox.

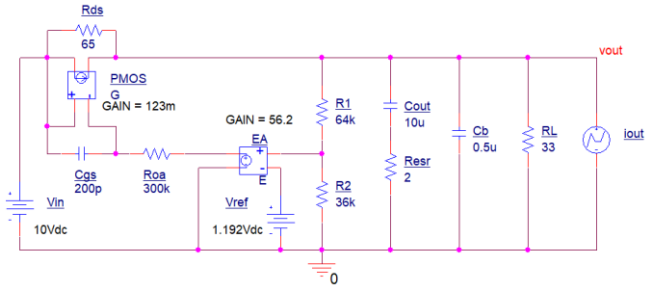

Figure 2: Test circuit

VR undershoot and overshoot can be mathematically computed from the VR output voltage, $v_{out}(s)$ the equation, derived from the small signal analysis, when all parameters inside the VR are known [6]. Undershoot is the difference between the initial and minimum values of the output voltage, while overshoot is the difference between the maximum and initial values of the output voltage. $v_{out}(s)$ is described as

$$v_{out}(s) = i_{out}(s)\, z_{out\_CL}(s), \tag{1}$$

where $i_{out}(s)$ is the load current with the small magnitude and typically changes abruptly and acts as the disturbance signal. $z_{out\_CL}(s)$ is the closed loop output impedance of VR. Figure 2 shows that $z_{out}(s)$ can be derived on the basis of the open loop output impedance of VR, $z_{out\_OL}(s)$, and open loop gain, $T(s)$, as shown in the following equations:

$$z_{out\_CL}(s) = z_{out\_OL}(s)\left(\frac{1}{1+T(s)}\right) \tag{2}$$

$$z_{out\_OL}(s) = R_{ds}||(R_1+R_2)||\left(\frac{1}{sC_{out}}+R_{esr}\right)||\frac{1}{sC_b}||R_L \tag{3}$$

$$T(s) = G_{FB}G_{EA}G_{PMOS}\left(\frac{1}{sC_{gs}R_{oa}}\right)\left(\frac{Z_1}{R_{ds}+Z_1}\right) \tag{4}$$

$$G_{FB} = \frac{R_2}{R_1+R_2} \tag{5}$$

$$G_{PMOS} = g_m R_{ds} \tag{6}$$

$$Z_1 = \left(\frac{1}{sC_{out}}+R_{esr}\right)||\frac{1}{sC_b}||R_L, \tag{7}$$

where G_{EA} is the error amplifier gain and g_m is the small signal transconductance of p-channel metal-oxide semiconductor (PMOS) transistor. Several parameters in Figure 2 are difficult to be accurately determined in the actual VR due to variations in the manufacturing process, such as R_{ds}, C_{gs}, and R_{oa}, which are drain-source resistance or output resistance of PMOS transistor, gate-source capacitance of PMOS transistor, and the output resistance of error amplifier, respectively. Therefore, the manual characterization was conducted to determine the VR stable region on the basis of actual VR circuit measurement.

Meanwhile, the VR output voltage during steady state, V_{OUT_SS}, which is the constant and stable output voltage before any disturbance signal was applied, can be defined as

$$V_{out\_SS} = V_{ref}\left(1+\frac{R_1}{R_2}\right). \tag{8}$$

C. Manual VR Characterization

After the circuit was developed, manual VR characterization was conducted to generate a stable region benchmark for the subsequent processes. The output current was configured between 10 and 250 mA, while the ESR range was from 0.1 to 100 Ω. Each combination of output current and ESR represents an operating point in the ESR tunnel graph. Manual characterization was completed after all operating points were tested.

In each operating point, the following processes were executed. First, the output current and ESR were configured before starting the characterization. Once started, the characterization time was recorded. Then, the circuit was simulated in OrCAD, and a circuit raw data file was exported into MATLAB. During the circuit simulation, the output current was changed abruptly to create a disturbance to the VR circuit.

Subsequently, the VR output responses, particularly undershoot of the VR output voltage, were analyzed. Thereafter, whether this undershoot was stable or unstable was determined on the basis of the VR datasheet. Finally, the ESR tunnel graph was plotted for each operating point under the stability condition. After simulation and analysis were completed, characterization time was stopped. Finally, a manual characterization dataset was developed.

D. Fully Data-Driven VR Characterization

As mentioned earlier, the newly proposed approach for characterization of VR stable region in this work is an FDD approach which utilized the RBFNN method. The overall process in the FDD approach involves a reduction in manual characterization dataset, RBFNN training, and stable region prediction using trained RBFNN.

The FDD approach utilized the dataset from manual characterization for RBFNN training. The number of data in the dataset was reduced to improve the characterization speed. In this case, only a certain number of operating points were required to acquire the data manually. Thereafter, the reduced dataset was divided into RBFNN training and testing datasets. In the FDD approach, the RBFNN inputs were output current and ESR while the RBFNN target was the VR undershoot. Figure 3 shows the VR modeling based on the proposed RBFNN.

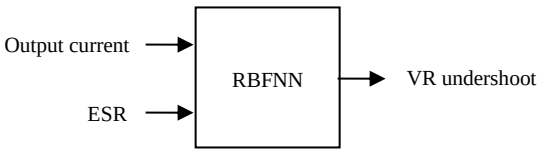

Figure 3: VR modeling using RBFNN

In this work, RBFNN was implemented to estimate the VR stable region. The approach was selected because of its simpler structure than that of another type of NN, namely, multilayer perceptron. Figure 4 shows the basic structure of RBFNN.

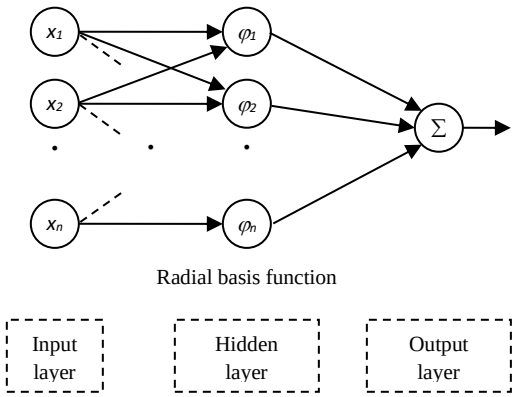

Figure 4: Basic internal structure of RBFNN

The RBFNN structure basically comprises input, hidden, and output layers. The input layer receives the external input signals and then redistributes these signals to the hidden layer. The hidden layer possesses nodes or neurons with a radial basis function (RBF). A typical RBF is the Gaussian function described as follows:

$$\varphi(x,\mu) = e^{\frac{||x-\mu||^2}{2d^2}}, \quad (9)$$

where: x = Input
μ = Mean or center of x
d = Spread of the Gaussian function

After the NN training was completed, the undershoot of VR output for the remaining operating points in the ESR tunnel graph was estimated. Subsequently, the ESR tunnel graph was plotted for the RBFNN approach. Finally, all stable region boundaries from the RBFNN approach were compared with the benchmark extracted from manual characterization. In addition, the characterization time was compared.

III. Results and Discussion

A. Results of Manual VR Characterization

As described earlier, the main aim of this work is to develop an efficient and effective characterization method. On the one hand, an efficient method is achieved if the developed method can reduce the characterization time. On the other hand, an effective characterization method is realized when the newly proposed approach presents a high stable region estimation accuracy. Therefore, a stable region benchmark extracted from manual characterization will be discussed first.

Figure 5 shows the ESR tunnel graph of manual characterization, and this graph acts as the benchmark in this work. Figure 5 indicates that three separate regions are found as follows: a stable region in the middle of the graph and two unstable regions. Clearly, two stability boundaries are obtained and considered the lower and upper ESR specification limits. The circle marks in Figure 5 indicate stable operating points, while the cross marks indicate unstable operating points. The ESR tunnel graph in Figure 5 is similar to the graph from the datasheet shown in Figure 1.

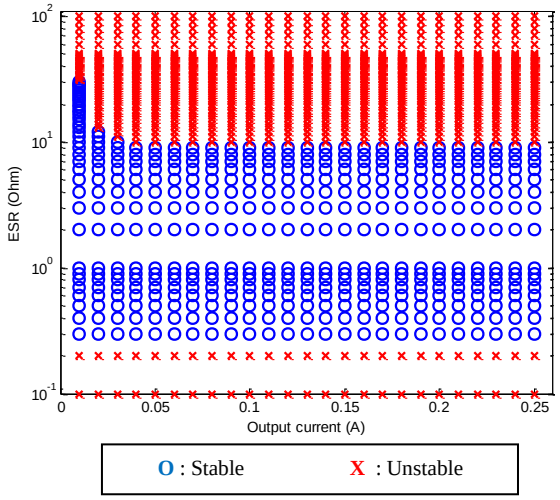

Figure 5: ESR tunnel graph of manual characterization

B. Results of Fully Data-Driven VR Characterization

After the stable region benchmark was determined, the RBFNN approach for VR characterization was conducted. Figure 6 shows the ESR tunnel graph of VR characterization using RBFNN. This result was obtained using the trained RBFNN structure with an RBF spread of 1.2 after testing for several spread values from 1.0 to 2.0 with an increment of 0.2.

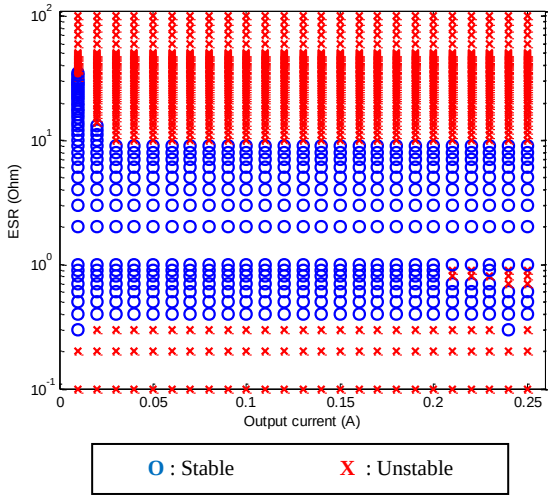

Figure 6: ESR tunnel graph of VR characterization using the fully data-driven approach

The ESR tunnel graph in Figure 6, which is the outcome of VR characterization using the RBFNN approach, presents a similar performance to the ESR tunnel graph of manual

characterization. This RBFNN result was obtained using a reduced number of the dataset with a reduction of 2. Figure 7 displays the comparison of stable regions from the manual characterization and VR characterization using the RBFNN approach. This comparison shows that the prediction accuracy of the RBFNN approach is 98.6% when estimating the upper ESR specification limit, which resides on the upper part of the stable region boundary in the ESR tunnel graph. Therefore, the proposed method can yield a reliable, stable region with few numbers of manual data acquisition.

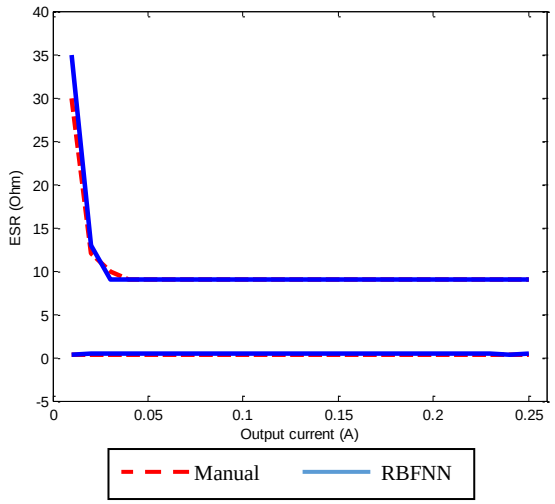

Figure 7: Comparison of stable region boundaries between manual characterization and RBFNN

C. *Characterization Time*

The total time for the RBFNN-based characterization was validated. The characterization time of the RBFNN approach is significantly reduced by 76% compared with that of manual characterization. This result demonstrates that the RBFNN approach is an efficient characterization method and obtains a reliable stable region.

IV. CONCLUSION

An improved VR characterization for estimating the stable region of VR in terms of ESR using the RBFNN approach was investigated in this work. The results of estimated stable regions show a good correlation with the benchmark from manual characterization. In other words, RBFNN-based VR characterization shortens the VR characterization process and effectively produces a reliable stable region.

ACKNOWLEDGMENTS

The authors acknowledge the financial support provided by the Universiti Kebangsaan Malaysia through research grant no. DIP-2015-012.

REFERENCES

[1] G. Rincon-Mora, *Analog IC Design with Low-Dropout Regulators (LDOs)*. United States of America: McGraw-Hill, 2009.

[2] T. Coulot, E. Lauga-Larroze, J. M. Fournier, M. Alamir, and F. Hasbani, "Stability analysis and design procedure of multiloop linear LDO regulators via state matrix decomposition," *IEEE Trans. Power Electron.*, vol. 28, no. 11, pp. 5352–5363, 2013.

[3] S. B. Nasir, S. Gangopadhyay, and A. Raychowdhury, "All-digital low-dropout regulator with adaptive control and reduced dynamic stability for digital load circuits," *IEEE Trans.Power Electron.*, vol. 31, no. 12. pp. 8293–8302, 2016.

[4] A. H. Musa, M. H. M. Zaman, R. Mohamed, and M. M. Mustafa, "Characterization of voltage regulators by automated equivalent series resistance," in *Proc. IEEE Conference on Systems, Process and Control (ICSPC 2014)*, 2014, pp. 68–72.

[5] *Robust Dimensioning of the Output Capacitor: Application Note*, Infineon, 2014.

[6] B. S. Lee, "Understanding the stable range of equivalent series resistance of an LDO regulator," *Analog Appl. J.*, pp. 14–17, Nov. 1999.

[7] A. M. Imam, "Real-time condition monitoring of the electrolytic capacitors for power electronics applications," in *Proc. Twenty-Second Annual IEEE Applied Power Electronics Conference and Exposition*, 2007, pp. 1057–1061

[8] G. A. Rincon-Mora and P. E. Allen, "A low-voltage, low quiescent current, low drop-out regulator," *IEEE J. Solid-State Circuits*, vol. 33, no. 1, pp. 36–43, 1998

[9] K. Harada, A. Katsuki, and M. Fujiwara, "Use of ESR for deterioration diagnosis of electrolytic capacitor," *IEEE Trans. Power Electron.*, vol. 8, no. 4, pp. 355–361, 1993.

[10] M. Dobler, M. Harrant, M. Rafaila, G. Pelz, W. Rosenstiel, and M. Bogdan, "Bordersearch: An adaptive identification of failure regions," in *Proc. 2015 Design, Automation & Test in Europe Conference & Exhibition (DATE 2015)*, 2015, no. 1, pp. 1036–1041

[11] "TPS76301, TPS76316, TPS76318, TPS76325, TPS76327, TPS76328, TPS76330, TPS76333, TPS76338, TPS76350 low-spower 150-mA low-dropout linear regulators data sheet," Texas Instruments, Texas, United States of America.